Observation and simulation of electrohydrodynamic instabilities in aqueous colloidal suspensions

Yue Hu, J. L. Glass, and A. E. Griffith
Department of Physics, Wellesley College, Wellesley, Massachusetts 02181

Seth Fraden
Martin Fisher School of Physics, Brandeis University, Waltham, Massachusetts 02254

(Received 24 September 1993; accepted 2 December 1993)

When an alternating linear electric field is applied to an aqueous suspension of micron-size polystyrene particles, hydrodynamic instabilities are seen at a frequency range between 2 and 200 kHz. The formation of elongated bands of particles oriented at certain angles relative to the direction of the applied electric field and circulation of particles within the bands are observed. We examine the phase lag between the induced dipole moments of the particles and the effects of this on the interactions between neighboring particles. Because the phase lag causes neighboring particles to exert torques upon one another, thereby causing spinning of double layers, we propose a phenomenological model in which there is a symmetry breaking between the direction of the polarization of the particles and the direction of the applied electric field. Based on this modified dipole–dipole interaction, and together with hydrodynamic interactions, we are able to simulate the formation of the tilted bands of particles. The sense of circulation of particles within a band also agrees with our experimental observations.

I. INTRODUCTION

The dramatic change in the rheological properties of colloidal suspensions under the influence of electric fields has attracted the attention of both the industrial and scientific communities since first discovered nearly half a century ago.[1] It has been generally understood[2] that when an electric field is applied to an electrorheological (ER) suspension, the particles in the suspension become polarized, acquiring induced dipole moments and attracting each other in the direction of the induced moments, which is parallel to the applied field. Chains and columns of the particles form as a result, thereby causing a drastic increase in the viscosity of the suspension.

These phenomena have recently been the subject of extensive theoretical and computer simulation work.[3,4] Because the dipole–dipole interaction is assumed to be the source of chain and column formation in all existing models, a clear understanding of the polarization of the particles and of the interactions between the particles is therefore crucial to the understanding of ER materials.

In order to gain more insight into the polarization and relaxation of colloidal particles, alternating electric fields have been used to measure the dielectric increment of bulk samples of particles in aqueous suspensions.[5,6] In addition, video technology has been used to study the dynamic process of particle association in electric fields in quasi-two-dimensional geometry.[7,8] Useful information on the relaxation time and pair interaction potential has been obtained through this work. However, since a charged colloidal particle in an aqueous solution attracts an ionic cloud of the opposite charge (*double layer*), the polarization of such a particle is far more complex than just a simple induced dipole moment. Over certain frequency ranges of the applied electric field, particles have been observed to rotate, indicating the exertion of torque on each other.[9] Furthermore, under favorable conditions, bands of particles have also been seen to form in directions other than that of the applied field, and there has also been circulation of particles within those bands.[10]

In explaining their experimental observation of these tilted bands, Jennings and Stankiewicz[10] have cited the competition between the electric potential energy of mutual polarization of two neighboring particles, which favors the particles lining up parallel to the direction of the applied field, and the fluid flow associated with the dynamic oscillation of particles in an alternating force field, which favors the particles lining up perpendicular to the applied field. A few crucial questions, however, remain unanswered. Clearly, the interactions between the particles in a tilted circulating band do not have the same symmetry as that of the applied linear field. How do we explain this symmetry breaking, and how do we explain the circulation of particles within a band?

In this paper, we will try to address these questions and propose a new model. Computer simulation results of this model will also be presented and will be compared with our experimental observations.

II. EXPERIMENTAL OBSERVATIONS

Our samples consisted of 1% volume-fraction suspensions of 1.5 μm-diameter monodisperse polystyrene spheres in an electrolyte of 2 mM KCl. The sample cell, as illustrated in Fig. 1, was made of two microscope slides sealed off with a round rubber O ring. A glass post was glued to the middle of one slide, providing an island of about 0.3 cm^2 area over which the sample was confined to a nearly two-dimensional space. The parallelism and the thickness of the gap could be adjusted by varying pressure on the screws that held the sample cell together while observing the pattern of interference fringes of light produced

 0021-9606/94/100(6)/4674/9/$6.00

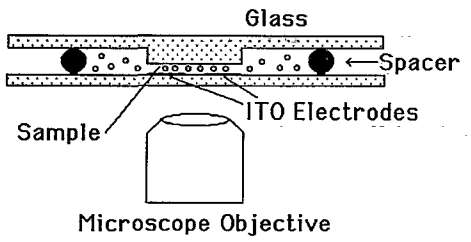

FIG. 1. A schematic of the side view of a sample cell.

by the gap. Directly above the post, the glass slide was coated with a thin layer of transparent indium–tin oxide conductor. The conductor was etched into two electrodes which could provide an electric field parallel to the surface of the glass. The electrodes were in direct contact with the sample, and the gap between them was about 0.5 mm. Homemade amplifiers, capable of delivering peak-to-peak voltages of up to 400 V from 2 kHz to 3 MHz, supplied an alternating voltage across the electrodes. The motion of particles between the electrodes in the two-dimensional region could be observed under an optical microscope, and the experiments could be recorded on videotape.

When the frequency of the applied field was greater than 200 kHz, particles lined up to form chains and columns, as expected for electric dipole interactions between the particles. At low frequencies, however, particles formed bands at nearly $\pm 45°$ relative to the direction of the applied field, as shown in Fig. 2. Within a band, particles were dynamically unstable, circulating in a counterclockwise direction if the band tilted to the right relative to the applied field and circulating clockwise if the band tilted to the left. There were isolated bands, and also bands tilted in opposite directions joined together at the ends. The speed of particle circulation was increased when the strength of the applied field was increased, and the circulation was also sensitive to the frequency of the field. Due to large energy dissipation and deterioration of electrodes at frequencies close to d.c., experiments were not carried out for frequencies below 2 kHz. However, down to the lowest frequencies we did test, the unstable motion and circulation of particles persisted.

Another interesting observation was that the particles seemed to be spinning. Even though we could not see the actual spinning of individual particles due to the optically isotropic nature of the spheres, the otherwise unexpected tangential movements of particles when they came into close contact strongly suggested such spinning motion.

III. MODEL

Based on these experimental facts, we realize that a successful model must be able to explain the asymmetry between the applied linear field and the tilted bands, as well as the circulation of particles within a band. We shall use earlier theoretical calculations on the polarization of dielectric spheres in aqueous solutions and then look into the

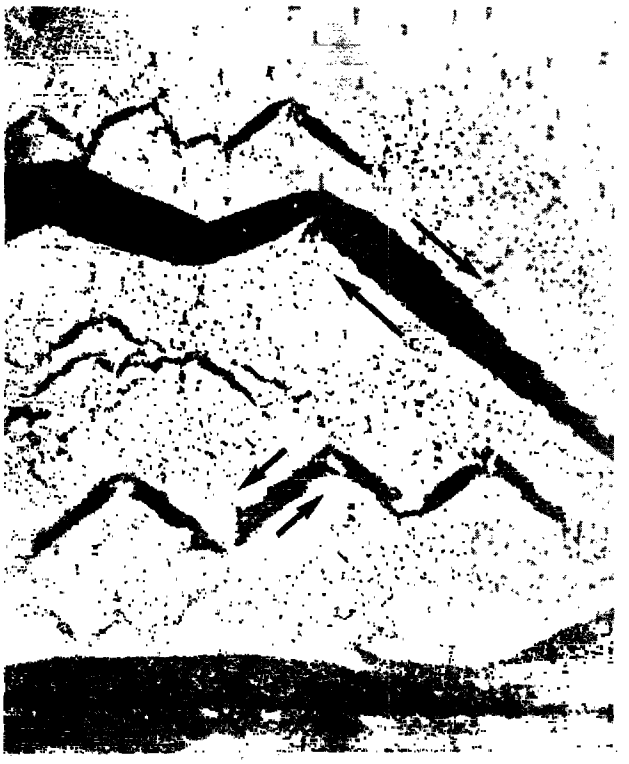

FIG. 2. The formation of diagonal bands of 1.5 μm polystyrene particles in an a.c. electric field at 145 kHz. The particles are suspended in an aqueous solution of 2 mM KCl. The lower horizontal dark band is the condensation of particles at the edge of one electrode. The applied electric field is in the vertical direction. Particles circulate in a counterclockwise sense in bands tilted to the right and circulate clockwise in bands tilted to the left.

interactions between two neighboring spheres. The consequences of these interactions will be discussed and a model based on the analysis will be proposed.

A. Polarization of a sphere

The polarization of a polystyrene sphere in an aqueous suspension by an alternating electric field can be understood in the following qualitative way: the dielectric constant of the sphere, typically about 2 to 3, is much smaller than that of water, which is about 80 in the frequency range of interest here. Therefore, the polarization of the sphere is that of a dielectric hole and is antiparallel to the direction of the applied field. A further complication is encountered, however, because the sphere is negatively charged, which attracts a cloud of positive ions (*counterions*). Close to the surface of the sphere, the counterions are tightly bound due to strong Coulombic forces. A few monolayers further from the sphere, the counterions are more loosely bound and form a diffuse layer. When an electric field is applied, the diffuse layer is distorted from a spherical shape and the charge distribution in the tightly bound layer is also altered. This nonspherical distribution of the double layer can be treated as an induced dipole moment which is parallel to the applied field.

We should point out that the distortion of a double

layer is sensitive to the frequency of the applied field. When the frequency is low, the counterions in the diffuse layer are displaced by a distance comparable to the size of the particle. The induced dipole moment is therefore very large and is parallel to the direction of the applied field. According to Lim and Franses' measurement of dielectric dispersion of bulk suspensions,[5] the central relaxation frequency of the diffuse layer of 1 μm polystyrene spheres is about 400 Hz, which is well below 2–200 kHz, the frequency range of electrohydrodynamic instability in our experiments. At the frequency range we are interested in, the shape of the diffuse layer does not have enough time to be distorted and therefore the polarization of the particle is more likely of Maxwell–Wagner type, which is due to the interfacial charges between two media of different dielectric constants and conductivities. Because of this, we can describe the polarization of a polystyrene sphere using analytic results derived by Schwarz,[11] which predict a Maxwell–Wagner type polarization modified by a tightly bound diffusive conducting surface layer.

In Schwarz's model, the motion of counterions around a spherical particle is characterized by the balance of two currents—one induced by the applied electric field, which deforms the spherical distribution of the ions, and the other governed by a diffusive process that tends to reestablish the spherical distribution. The total induced dipole moment is

$$\mu=4\pi\epsilon_0\epsilon_s\frac{\epsilon_p^*+\Delta\epsilon_p-\epsilon_s^*}{\epsilon_p^*+\Delta\epsilon_p+2\epsilon_s^*}R^3E, \tag{1}$$

where R is the radius of the particle, E is the strength of the applied electric field, ϵ_0 is the permittivity constant, and ϵ_p^* and ϵ_s^* are the complex dielectric constants of the particle and of the solvent, respectively. [In an alternating electric field of form $E_0e^{i\omega t}$, the complex dielectric constant ϵ^* is related to the real dielectric constant ϵ by

$$\epsilon^*=\epsilon-i\kappa/(\omega\epsilon_0), \tag{2}$$

where κ is the conductivity and ω is the angular frequency of the applied field.] $\Delta\epsilon_p$ is the increment in the dielectric constant of the particle due to the polarization of the diffuse layer and has a Debye-type dispersion

$$\Delta\epsilon_p=\frac{1}{1+i\omega\tau}\frac{e_0^2R\sigma_0}{\epsilon_0kT}, \tag{3}$$

where e_0 is the charge of a counterion, σ_0 is the surface charge density (ions per unit area), k is Bolzmann's constant, and T is the temperature. We should point out that the magnitude of $\Delta\epsilon_p$ may become much larger than that of ϵ_p^* at low frequencies. The relaxation time τ is related to the mechanical mobility u (velocity per unit force) of a counterion and to its diffusion constant D by

$$\tau=\frac{R^2}{2ukT}=\frac{R^2}{2D}. \tag{4}$$

We can see that τ is on the order of the time required for a counterion to diffuse the length of a particle.

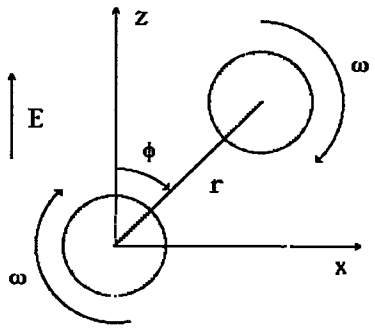

FIG. 3. Two neighboring spheres exert net torque on each other due to the phase lag between the induced dipole moments and the applied electric field.

An important feature of Eq. (1) is the phase lag between the induced dipole moment and the applied electric field. We also note that this phase lag depends on the frequency of the applied field, and this is in fact very similar to an overdamped oscillator in a periodic force field. In general, there is a phase shift between the response of the oscillator and the driving force and, as we shall see later, this phase shift plays a crucial role in our model and in explaining our experimental observations.

B. Mutual polarization between two neighboring spheres

We now consider two neighboring particles separated by a distance r. The applied electric field is linear and sinusoidal, pointing in the z direction. As illustrated in Fig. 3 the line connecting the centers of the two particles is oriented at an angle ϕ relative to the z axis. As a first-order approximation, the polarization of each particle is treated as a point dipole located at the center of the sphere. The induced dipole moment is proportional to the applied electric field in strength, but lags behind in time, as discussed in the previous section. We denote this phase shift explicitly by θ, i.e., $\mu\propto Ee^{-i\theta}$.

Because the field created by a dipole falls off as the inverse cube of the distance, we only consider mutual polarization to first order, i.e., when considering the field created by particle 2 at particle 1, instead of using the net dipole moment of particle 2 induced by its total local field, we only use the leading term in its dipole, which is induced by the applied field. Doing this, we can easily calculate the electric potential energy of the pair

$$U=-\frac{F_0R}{3}\frac{3\cos^2\phi-1}{r^{*3}}(1+\cos 2\theta), \tag{5}$$

with

$$F_0=6\pi\epsilon_0\epsilon_sR^2\beta^2E_0^2, \tag{6}$$

$$\beta=\left|\frac{\epsilon_p^*+\Delta\epsilon_p-\epsilon_s^*}{\epsilon_p^*+\Delta\epsilon_p+2\epsilon_s^*}\right|, \tag{7}$$

$$r^*=\frac{r}{R}, \tag{8}$$

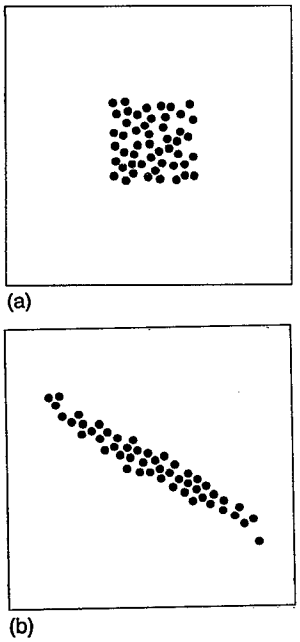

FIG. 4. (a) The initial configuration of 50 particles randomly placed within a square region. (b) The formation of a tilted circulating band after 1 000 000 time steps. The applied field is in the vertical direction. Simulation parameters are given in the text.

where E_0 is the root-mean-square amplitude of the applied field. We note that Eq. (5) has the familiar form of dipole–dipole potential energy except for a factor of $(1+\cos 2\theta)$, which is due to the phase shift between the induced dipole and the applied field. What is more interesting, however, is that the time-averaged torque exerted on each particle is nonzero due to this phase shift

$$M=-F_0R\frac{2\sin\phi\cos\phi}{r^{*3}}(1-\cos 2\theta). \tag{9}$$

This means that if two particles are not aligned parallel or perpendicular to the direction of the applied field, they will spin, and this has indeed been experimentally observed in biological cells.[9]

We should point out, however, that a torque of the form in Eq. (9) does not guarantee spinning because, as we can see from Eq. (5), the minimum energy state is achieved when the two particles are aligned with the applied field ($\phi=0$), and there is then no torque in this configuration according to Eq. (9). Therefore, to fully explain the experimental observations, one needs to justify why the particles prefer to align in a diagonal direction. In this paper, we present a phenomenological model to address these issues by further exploring the consequences of the spinning of particles.

Now we assume that when the field is turned on, two particles happen to be in the configuration shown in Fig. 3 ($0°<\phi<90°$). Then both particles will spin clockwise according to Eq. (9). As we know from fluid dynamics, when a sphere spins in a viscous fluid, the boundary layer of the fluid spins with the sphere, as required by boundary conditions. This means that *double layers spin with the particles*. Thus, when a linear alternating electric field is applied, the counterions no longer flow uniformly around a sphere because of a preference to flow with the spinning double layer, resulting in an induced dipole moment that is not in the same direction as the applied field. When the particles spin in a clockwise direction, as in Fig. 3, the induced dipole moments are tilted to the right relative to the applied field, causing them to stay aligned in that direction. We believe that this is the reason for the symmetry breaking between the applied field and the induced dipole moments.

We can present the above analysis in a more quantitative manner, similar to the treatment of the propagation of linearly polarized light in an optically active medium. We first express a linear alternating field as a sum of left and right circularly polarized fields, with each field inducing a dipole moment. As discussed in the previous paragraph, the phase shifts of the left and the right circularly polarized dipoles are different due to the rotation of the double layer. The combined net dipole moment is still linear, but pointing in a direction different from that of the applied field. The polarization is related to the applied field by a rotation tensor

$$\begin{pmatrix}\mu_x\\ \mu_z\end{pmatrix}\propto e^{-i\bar{\theta}}\begin{pmatrix}\cos\frac{\Delta\theta}{2} & \sin\frac{\Delta\theta}{2}\\ -\sin\frac{\Delta\theta}{2} & \cos\frac{\Delta\theta}{2}\end{pmatrix}\begin{pmatrix}E_x\\ E_z\end{pmatrix}, \tag{10}$$

with

$$\bar{\theta}=\frac{\theta_L+\theta_R}{2}, \tag{11}$$

$$\Delta\theta=\theta_L-\theta_R, \tag{12}$$

where θ_L and θ_R are the phase lags of the left and right circularly polarized dipoles.

By taking the negative gradient of the potential energy, we can calculate the electric forces between a pair of dipoles [shown in Fig. 3 and characterized by the polarization matrix of Eq. (10)]. When normalized to F_0, the radial and tangential components of the force on the particle at the origin are

$$f_r^{*el}=\frac{1}{r^{*4}}\left[3\sin\phi\cos\phi\sin\Delta\theta+(3\cos^2\phi-1)\cos^2\frac{\Delta\theta}{2}(1+\cos 2\bar{\theta})+(3\sin^2\phi-1)\sin^2\frac{\Delta\theta}{2}(1-\cos 2\bar{\theta})\right], \tag{13}$$

$$f_\phi^{*el}=\frac{1}{r^{*4}}\left[(2\sin^2\phi-1)\sin\Delta\theta+\sin 2\phi(\cos\Delta\theta+\cos 2\bar{\theta})\right]. \tag{14}$$

C. Hydrodynamic forces between two rotating spheres

The torque on the particles shown in Fig. 3 can also be calculated by taking the cross product of the induced di-

pole moments and the local field. A sphere of radius R rotating at angular velocity Ω in a fluid of viscosity η experiences a frictional torque

$$M_{\text{fric}}=-8\pi\eta\Omega R^3. \tag{15}$$

When the electric and the frictional torques are balanced, the normalized angular velocity of a particle is

$$\omega^*=\frac{1}{2\beta}\cos\bar{\theta}\sin\frac{\Delta\theta}{2}+\frac{1}{2r^{*3}}\left[3\sin\phi\cos\phi(\cos 2\bar{\theta}-\cos\Delta\theta)+\frac{3\sin^2\phi-1}{2}\sin\Delta\theta(\cos 2\bar{\theta}-1)+\frac{3\cos^2\phi-1}{2}\sin\Delta\theta(\cos 2\bar{\theta}+1)\right], \tag{16}$$

where time t is normalized relative to

$$t_0=6\pi\eta R^2/F_0. \tag{17}$$

We note that t_0 is independent of particle size since F_0 is proportional to R^2.

From fluid dynamics, we know that when a sphere spins at an angular velocity Ω in an infinite fluid of viscosity η, the fluid around it flows with a tangential velocity

$$v_\phi=\frac{R^3}{r^2}\Omega. \tag{18}$$

When considering the hydrodynamic interaction between two rotating spheres, we make a crude approximation by assuming that between the two spheres, the velocity of the fluid along the line connecting the centers of the spheres is a linear combination of the velocities of the fluid that would be induced by each individual sphere if the other sphere were absent. The velocity of the fluid at the boundary of each sphere along this line is matched to the velocity of the sphere, and we assume an effective interaction area A_{eff} to be on the order of a few tenths of R^2. If particles 1 and 2 rotate at angular velocities ω_1^* and ω_2^*, the tangential hydrodynamic force exerted on particle 2 on particle 1 (at $r=0$) is

$$f_{\phi 12}^{*\text{hyd}}=\frac{A_{\text{eff}}^*}{3\pi}\frac{\alpha^2(\omega_1^*\alpha^2+\omega_2^*)}{(1+\alpha^2)(1-\alpha)}, \tag{19}$$

where

$$\alpha=\frac{1}{r^*-1}. \tag{20}$$

D. Net force and the motion of a sphere

Besides the forces discussed above, there is also a short-range repulsive force between two particles in close contact due to the counterions. We assume a repulsive force of an exponential form

$$f_r^{*\text{rep}}=-200\exp[-(r^*-2)/0.05], \tag{21}$$

where the parameters have been chosen such that when the attractive dipole force is added, the equilibrium gap between two particles is about 15% of the diameter of the particles, matching our experimental observations.

Finally, we need to take into consideration a Stokes hydrodynamic drag force

$$F^{\text{hyd}}=-6\pi\eta R\mathbf{v}, \tag{22}$$

where $\mathbf{v}$ is the velocity of the particle. We should point out that because the particles in our experiments were confined between two stationary walls, the actual drag forces due to translational and rotational motion of a particle should be larger than the Stokes forces used in our model.[12] However, due to the phenomenological nature of the model, overlooking these details does not jeopardize the main objectives of this work. Brownian forces can also be safely neglected because dipolar potential energy is much stronger than the thermal energy under our experimental conditions.[2]

The dynamic equation for the ith particle can now be written as

$$m\frac{d^2\mathbf{x}_i}{dt^2}=\sum_{j\neq i}F_{ij}^{\text{el}}+\sum_{j\neq i}F_{ij}^{\text{rep}}+\sum_{j\neq i}F_{ij}^{\text{hyd}}+F_i^{\text{hyd}}, \tag{23}$$

where $\mathbf{x}_i$ is the position of the particle and m is its mass. If we use normalized position, time, and forces, the coefficient of the inertia term on the left side of the above equation becomes

$$m^*=\frac{m\epsilon_0\epsilon_s\beta^2E_0^2}{6\pi\eta R}, \tag{24}$$

which is on the order of 10^{-6}. This is sufficiently small compared to the coefficients of other terms that the inertia term can be safely ignored.

The last term in Eq. (23) is the Stokes drag force, which is proportional to the velocity of the ith particle. The other three force terms arise from pair interactions and are determined by the relative positions of particles in the system [as expressed by Eqs. (13), (14), (19), and (21)] and by $\Delta\theta$, the asymmetry in the phase lags of the left and right circularly polarized induced dipoles. The magnitude of $\Delta\theta$ is obviously related to the speed of spinning of the particle, which in turn is determined by the positions and phase shifts of the particle's neighbors. Because the equations are coupled and transcendental, we use a "mean-field" approximation, i.e., we assume that every particle has the same phase shift $\Delta\theta$. Judging from our experimental observations, this is not an unreasonable approximation for those particles in a single tilted band, because even though the particles are not in stable equilibrium, they do circulate within a band in an orderly fashion. Therefore, it is possible that they have phase shifts that are approximately uniform within a band. We treat $\Delta\theta$ as a variable parameter in our computer simulation work.

Keeping all this in mind, and using normalized units and setting the inertia term to zero, we can rewrite Eq. (23) as

$$\frac{d\mathbf{x}_i^*}{dt^*}=\sum_{j\neq i}f_{ij}^{*\text{el}}+\sum_{j\neq i}f_{ij}^{*\text{rep}}+\sum_{j\neq i}f_{ij}^{*\text{hyd}}. \tag{25}$$

This enables us to calculate the change of position of each particle from the ensemble configuration.

IV. COMPUTER SIMULATION RESULTS AND DISCUSSION

The initial configuration was comprised of 50 particles randomly positioned in a square region [Fig. 4(a)]. The applied electric field was in the vertical direction and the motion of particles was confined to two dimensions. Because the particles of interest in our experimental setup were not directly surrounded by the electrodes that supply the electric field, we did not need to be concerned with image charges and therefore did not impose boundary conditions on the particles. The interactions between particles were assumed to be pair interactions, as discussed in the previous section.

For every configuration of particles, the velocity of each particle was calculated according to Eq. (23), and a new configuration, after time step Δt^*, was computed for the next round of calculations. A typical time step was 0.01 and a total of 1 million particle configurations were usually calculated for each simulation run, typically taking about 8 h of computation time on an IBM RISC 6000 workstation. Using smaller Δt^* did not change the results of the simulation. The cut-off distance for the electric forces was 12, but due to the crudeness of our approximation, the cut-off distance for the hydrodynamic forces between a pair of spinning particles was only 4 because a longer cut-off distance had little meaning.

As discussed earlier, the polarization of a particle at the low-frequency limit is dominated by the double layer, so the strength of polarization should be about 1 according to Eq. (1) (in normalized units). At the high-frequency limit, the dielectric polarization dominates and the strength of polarization is about -0.5. Because we expected the situation we were dealing with to occur in the dispersive region of the polarization of the particle, we assumed the magnitude of the polarization strength (β) to be 0.1. We also assumed the effective area (A^*_{eff}) for hydrodynamic interaction between two spinning particles to be 0.2. Different values of average phase shift ($\bar{\theta}$) and phase asymmetry ($\Delta\theta$) were tried for the best agreement with our experimental observations.

Figure 4(b) shows the formation of a tilted band of particles for $\bar{\theta}=130°$ and $\Delta\theta=60°$. The particles within the band circulate in a clockwise sense. The shape of the band closely resembles the experimental results shown in Fig. 2, and the sense of circulation also agrees with experimental observations. The circulation of particles can be quantitatively characterized by an angular momentum

$$\mathbf{L}=\sum_i \mathbf{r}_i'^*\times\mathbf{v}_i'^*, \tag{26}$$

where the primes indicate that the corresponding quantities are measured in the center-of-mass frame. Figure 5 shows the time evolution of the angular momentum.

Our computer simulation program also kept track of the average root-mean-square velocity (in the laboratory frame) and the angular velocity of the spin of the particles. If we substitute into Eq. (17) parameter values appropriate for our experimental conditions (an electric field strength of about 1000 V/cm and water viscosity of about 10^{-3} N s/m^2), t_0 is about 30 ms. Converted to real time, the average translational velocity of a particle is on the order of one particle length per second, which is within the range of our experimental observations. The rotational speed of a particle is about 100 rad/s, which can be compared with the experimental results of Vienken and Zimmermann.[9] They measured the rotational speed of biological cells in aqueous solutions in alternating electric fields and obtained a rotational speed of about 1 rad/s at a field strength of 100 V/cm. Even though the colloidal particles in their system were different from ours, an order-of-magnitude comparison is still valid. According to Eqs. (6), (16), and (17), the rotational speed of a particle is proportional to the square of the field strength, but is independent of the particle size. Our experimental field strength is about ten times as strong as theirs and therefore a rotational speed 100 times as theirs is not unreasonable.

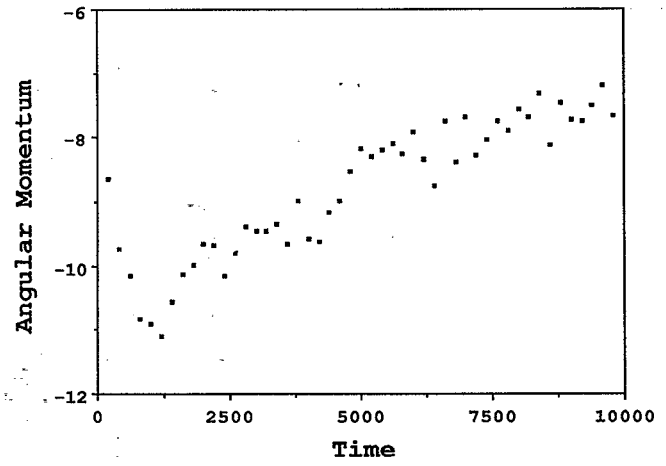

FIG. 5. Time evolution of the angular momentum of the system [defined by Eq. (25)] for the simulation run depicted in Fig. 4. The negative sign of the angular momentum indicates the circulation of the particles is clockwise.

We can also calculate the linear velocity of the double layer due to the rotation of a particle and compare this with the mobility of counterions. Using the numbers discussed in the previous paragraph, the linear velocity of the periphery of a particle (ωR) is on the order of 10^{-2} cm/s. The mobility of a typical free ion in solution (u_0) is about 10^{-4} cm s^{-1}/V cm^{-1}. For an ion in a double layer, its mobility is reduced due to electrostatic interaction with surface ions on the particle. The actual mobility is

$$u=u_0 e^{-\alpha/kT}, \tag{27}$$

where the activation energy α is on the order of 1 kcal/mol.[11] The velocity of a counterion in a field of strength 1000 V/cm is therefore on the order of 10^{-2} cm/s, comparable to ωR. This explains the large asymmetry ($\Delta\theta$) between the direction of the induced dipole moment and that of the applied field.

In explaining their experimental observation of tilted bands of circulating particles, Jennings and Stankiewicz[10] noted that two particles driven by a sinusoidal force interact with an effective potential

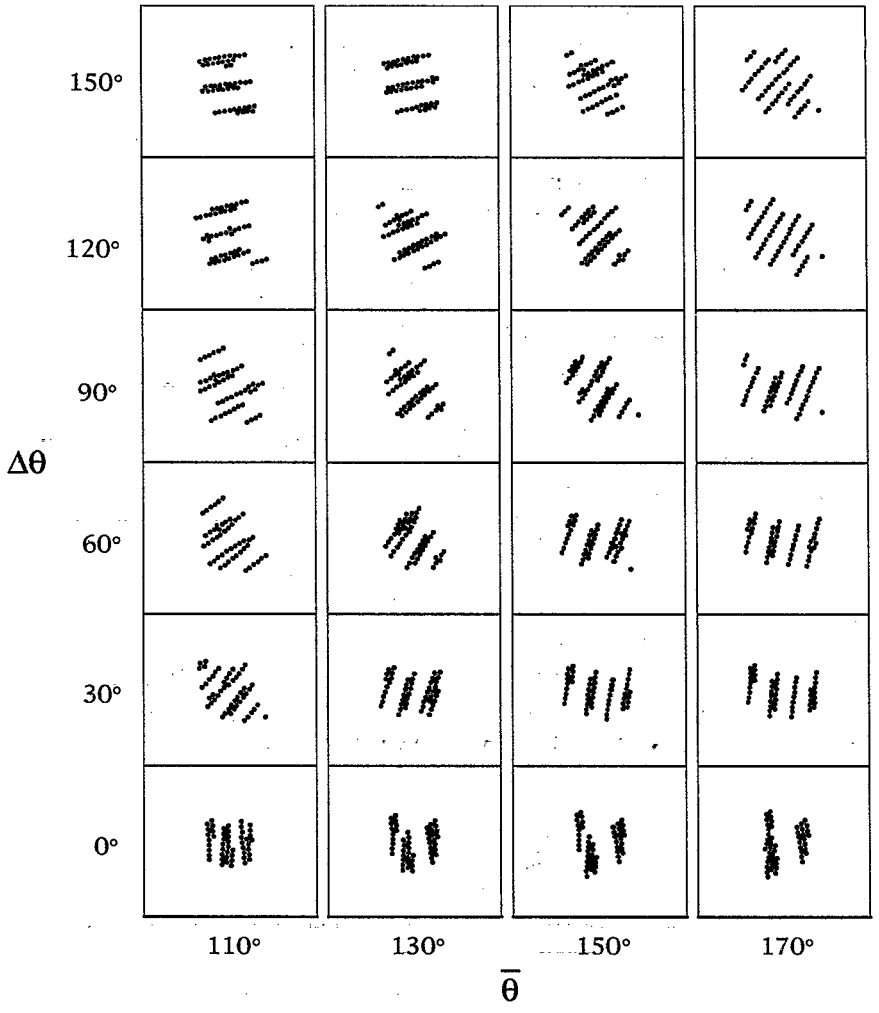

FIG. 6. Particles do not form tilted circulating bands if the hydrodynamic interaction due to spinning of particles is ignored ($A_{\text{eff}}=0$), even though the asymmetry between the induced dipole moment and the applied field is taken into consideration ($\Delta\theta\neq 0$).

$$U \propto \frac{3\cos^2\phi - 1}{r^3}, \tag{28}$$

which has the same dependence on r and ϕ as the electric potential energy of two dipoles, but which is opposite in sign. The competition between these two potential energies causes two particles to line up either parallel (when the electric potential dominates) or perpendicular to the applied field (when the mechanical potential dominates), but this does not explain the diagonal alignment of the particles. If it does play a significant role in the interactions between particles, we can treat it as a factor that reduces the strength of the electric potential energy. Because in our model all quantities are scaled to be dimensionless, the final outcome does not rely on the absolute value of the strength of polarization. Therefore, we did not include this mechanical potential energy in our model.

We performed numerous computer simulation runs with different values for A_{eff}, $\Delta\theta$, and $\bar{\theta}$ to find out the roles played by these parameters in the formation of tilted circulating bands of particles. By setting $A_{\text{eff}}=0$, but keeping other simulation parameters unchanged, we effectively ignored the spinning of particles by eliminating the hydrodynamic effect due to the spinning. As shown in Fig. 6, when A_{eff} was set to 0, we saw neither the formation of narrow bands nor the circulation of particles, but instead saw only the formation of chains and columns of particles which were almost motionless after a long time, as expected for electric interactions between fixed induced dipoles. The orientation of these chains and columns, which indicated the direction of minimum potential energy, was tilted away from the direction of the applied field if $\Delta\theta\neq 0$. This told us that with only an asymmetry between the induced dipole moment and the applied field, but with no spinning of particles, the formation of a tilted narrow band of particles could not be realized. On the other hand, if we only included the spinning of particles, but did not include the asymmetry between the induced dipole moment and the applied electric field (by setting $\Delta\theta=0$, but $A_{\text{eff}}\neq 0$), then we still did not see the formation of a tilted band (Fig. 7).

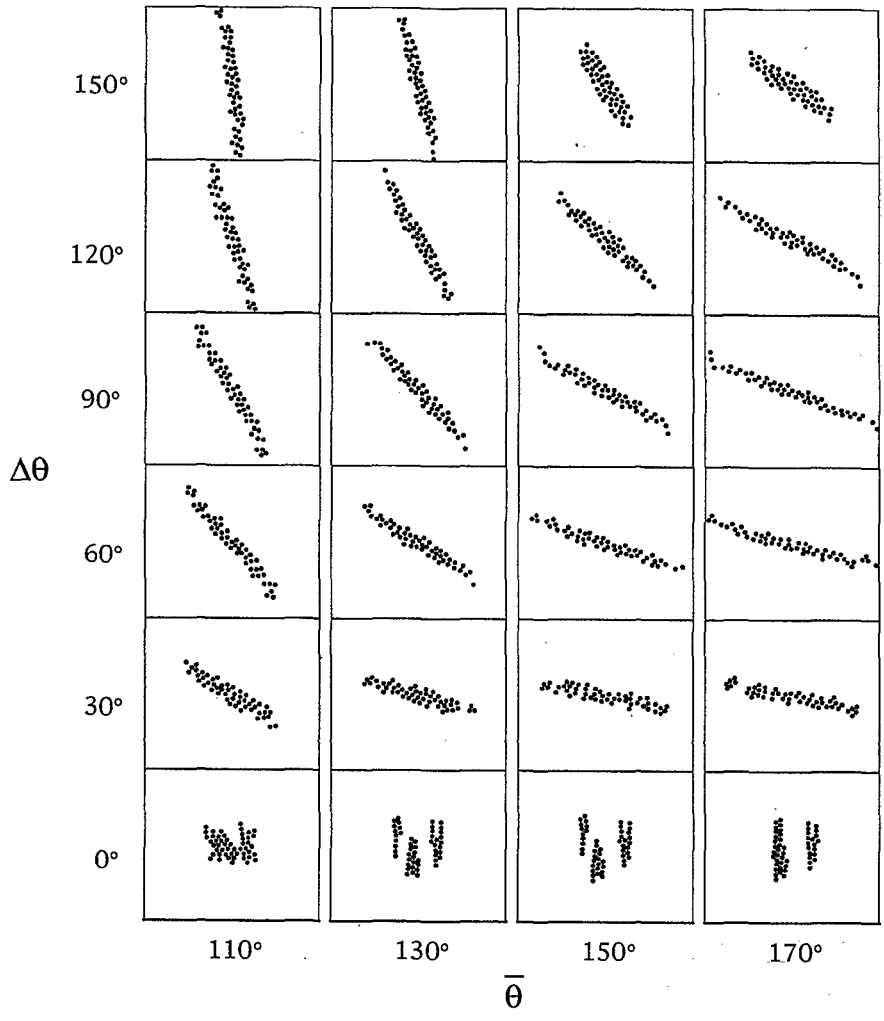

FIG. 7. In the bottom row, particles do not form tilted circulating bands when the asymmetry between the induced dipole moment and the applied field is ignored ($\Delta\theta=0$), even though the hydrodynamic interaction due to spinning of particles is included in the pair interaction ($A_{\text{eff}}\neq 0$). However, when both the asymmetry and the hydrodynamic interaction are included, particles form tilted circulating bands.

Another interesting fact is that the band tilted to the left while the electric dipole interaction between a pair of particles should have preferred an alignment with particles tilted to the right (because $\Delta\theta>0$). This seemed to have been the result of hydrodynamic interaction. When we set $A_{\text{eff}}=0$, then we saw the formation of almost stationary chains of particles tilted to the right. As we increased the effect of hydrodynamic interaction between the spinning particles by increasing the value of A_{eff} the length of the chains got shorter and instability became apparent. This seemed to be a tradeoff between minimizing the electric potential energy and reducing frictional loss due to shear forces between spinning particles. Electric dipole potential is minimized when particles form chains in the direction of the dipole moment. Those chains also attract each other sideways, forming columns.[13] Because the distance between neighboring particles within the same chain is shorter than the distance between two adjacent chains, the shear force is also greater between particles in a chain. To minimize the shear loss, chains along the direction of dipole moment become shorter and short chains are attracted sideways to form a band.

V. CONCLUSIONS AND FUTURE WORK

Our simulation results show that there are two key factors for the formation of tilted circulating bands of colloidal particles in linear alternating electric fields: (1) the asymmetry between the orientations of the induced dipole moments of the particles and the applied electric field, which causes the tilting angle of the band; and (2) tangential hydrodynamic forces due to the spinning of particles, which cause the circulation of particles within a band. If either of these two factors is absent, the formation of tilted circulating bands cannot be realized.

The misalignment between the induced dipole of a particle and the linear applied field can be explained by our phenomenological model. In this model, mutual polarization of neighboring particles causes spinning of particles due to the phase lag between the polarization and the ap-

plied field. The spinning of a particle breaks the symmetry between the flow of counterions in the double layer and the applied field and thereby produces a dipole that is not oriented in the same direction as the applied field.

Unfortunately, we could not simulate the spontaneous symmetry breaking between the direction of induced dipole moments and that of the applied field because we employed a fixed $\Delta\theta$ for each simulation run (mean-field approximation). In real experiments, this symmetry breaking is a gradual process. The formation of tilted bands of circulating particle does not occur until a few minutes after the field is turned on. Therefore, our model is only valid for the time region after the symmetry breaking has occurred. We will leave the simulation of spontaneous symmetry breaking for future work. In future experiments, we will try to detect the spinning of particles, possibly by using particles that are slightly asymmetrical. We will also simultaneously measure dielectric dispersion and observe the motion of particles, so that we can correlate dispersion with particle motion.

Our formulation of the hydrodynamic interaction between particles is almost certainly oversimplified because the particles are not in a three-dimensional geometry, and superposition of pair hydrodynamic interactions when particles are in close proximity is also problematic. Nevertheless, we feel confident that the shear force between spinning particles is qualitatively correct because an effective interaction area (A_{eff}) of $0.2R^2$ is very reasonable.

We should emphasize the phenomenological nature of our model. The simulation parameters are by no means matched to the true experimental values because there are too many unknown components. Nevertheless, we believe that our model captures the essence of the electric and hydrodynamic interactions between colloidal particles in aqueous suspensions in certain frequency ranges because the qualitative agreement between our simulation results and experimental observations is good.

ACKNOWLEDGMENTS

Y.H. gratefully acknowledges the support of a Clare Boothe Luce Professorship funded by the Henry Luce Foundation, as well as the support of the National Science Foundation (grant no. DMR-92-12090). S.F. acknowledges research support from Brandeis University, where the experimental work was performed. J.L.G. and A.E.G. acknowledge Undergraduate Summer Research Awards funded by the Howard Hughes Medical Institute and by Wellesley College. We would also like to thank the Computer Science Department of Wellesley College for the use of their computers, and J. L. Sánchez for programming assistance.

[1] W. M. Winslow, J. Appl. Phys. **20**, 1137 (1949).
[2] A. P. Gast and C. F. Zukoski, Adv. Colloid Interface Sci. **30**, 153 (1989).
[3] D. J. Klingenberg, Frank van Swol, and C. F. Zukoski, J. Chem. Phys. **91**, 7888 (1989); **94**, 6160 (1991); **94**, 6170 (1991).
[4] R. T. Bonnecaze and J. F. Brady, J. Chem. Phys. **96**, 2183 (1992).
[5] K. H. Lim and E. I. Franses, J. Colloid Interface Sci. **110**, 201 (1985).
[6] J. Lyklema, M. M. Springer, V. N. Shilov, and S. S. J. Dukhin, Electroanal. Chem. **198**, 19 (1986).
[7] S. Fraden, A. J. Hurd, and R. B. Meyer, Phys. Rev. Lett. **63**, 2373 (1989).
[8] P. M. Adriani and A. P. Gast, Faraday Discuss. Chem. Soc. **90**, 17 (1990).
[9] C. Holzapfel, J. Vienken, and U. Zimmermann, J. Membrane Biol. **67**, 13 (1982).
[10] B. R. Jennings and M. Stankiewicz, Proc. R. Soc. London Ser. A **427**, 321 (1990).
[11] G. Schwarz, J. Phys. Chem. **66**, 2636 (1962).
[12] J. Happel and H. Brenner, *Low Reynolds Number Hydrodynamics* (Kluwer, Dordrecht, 1991).
[13] T. C. Halsey and W. Toor, Phys. Rev. Lett. **65**, 2820 (1990).